Epitaxial growth of Cr on Ag(001)

P. Steadman,* C. Norris, C. L. Nicklin, N. Jones, and J. S. G. Taylor
Department of Physics and Astronomy, University of Leicester, Leicester, LE1 7RH, United Kingdom

S. A. de Vries†
FOM-Institute for Atomic and Molecular Physics, Kruislaan 407, 1098 SJ Amsterdam, The Netherlands

S. L. Bennett
CCLRC Daresbury Laboratory, Warrington, Cheshire, WA4 4AD, United Kingdom
(Received 22 June 2001; revised manuscript received 24 September 2001; published 3 December 2001)

The growth morphology and structure of ultrathin films of Cr deposited on Ag (001) have been studied *in situ* by surface x-ray diffraction. The reflected x-ray intensity at the anti-Bragg position along the $(00l)$ rod was monitored during growth at temperatures between 100 and 473 K. At room temperature, there is a steady decay of the intensity, indicative of disordered growth. At higher temperatures the variation of the intensity with time is consistent with the coating of monolayer platelets of Cr with Ag. At 100 K weak oscillations were observed, which decayed relatively quickly. Scans along the reciprocal-lattice vectors perpendicular to the surface were recorded for three different coverages. Expanded interface spacings were found in all of the films. For the two films grown at 100 K analysis of the scans indicated that a fraction of the films were disordered. The Cr film grown at a temperature of 430 K was found to intermix with the layer of Ag that covers it.

DOI: 10.1103/PhysRevB.64.245412 PACS number(s): 68.55.−a

I. INTRODUCTION

There has been considerable interest in the properties of ultrathin metal films supported on oriented single-crystal surfaces. The reduced symmetry and atomic coordination modify the overlap of the atomic orbitals and, in consequence, change the magnetic properties. Giant moments, perpendicular magnetic anisotropy, and giant magnetoresistance are some of the effects that have been attributed to reduced dimension.[1–3] The change in magnetic behavior at a surface and in ultrathin films can be related in part to the increase in the volume of the unit cell and a narrowing of the electronic valence bands at the Fermi level.[2]

Since Cr has a half filled 3*d* band it should be extraordinary sensitive to changes in coordination and symmetry. Enhanced moments from that of the bulk[4] have been calculated and found for both the Cr surface[5–8] and Cr thin films.[9–13] In one study, polarized neutron reflection measurements of a 0.33 monolayer film deposited on Ag(001) were consistent with ferromagnetism and not antiferromagnetism as found in the bulk.[12] A full potential linearized augmented plane wave (FLAPW) study of monotonic multilayer Cr/Ag structures predicts an antiferromagnetic ground state for the Cr layers with large local moments.[14,15]

A better understanding of the magnetic properties observed with ultrathin films necessarily demands knowledge of the detailed atomic structure and a high degree of control of the growth. Cr on Ag(001) would appear to be an attractive candidate for study and was one of the first systems to be measured.[11] The nearest-neighbor separation in fcc Ag (2.89 Å) is only 0.2% greater than the lattice parameter of bcc Cr (2.88 Å) and the Cr-Ag binary system has a large miscibility gap above the melting point.[16] We would, therefore, expect the bulk Cr phase to grow epitaxially on the Ag(001) surface (with the [100] axis rotated by 45° relative to the substrate) with good order and little intermixing of the species at the interface. Against this, the significantly greater surface free energy of Cr (2400 mJ/m^2) in comparison with that of Ag (1250 mJ/m^2) implies that a Cr layer on top of a Ag substrate is energetically unfavorable and would only form under nonequilibrium conditions.

There have been several studies of the adsorption of Cr on Ag(001) that suggest that the growth is nonsimple. Newstead *et al.*[11] proposed that, at room temperature, the growth initially proceeds by the formation of monolayer islands with perfect epitaxy. At approximately $\frac{1}{3}$ ML, bilayers are formed and beyond 2 ML the growth is disordered. Angle-resolved Auger measurements by Johnson *et al.* showed that the structure of the Cr overlayer was a rotated bcc structure as expected.[12] Krembel *et al.*[17–20] confirmed that, at room temperature, a mixture of monolayers and bilayers occurs at one monolayer coverage; above 460 K, three-dimensional islands were formed. Surprisingly, in a narrow temperature range (430–450 K) and at relatively low deposition rates, evidence was found of a flat metastable layer. It was suggested that the layer could have been stabilized by two-dimensional antiferromagnetic order. An alternative explanation proposed the existence of a two-dimensional Cr-Ag alloy despite the mutual immiscibility of this system.[10] The formation of a surface alloy of constituents that do not mix in the bulk has been reported for several systems (for examples, see Refs. 21–23). In another study, Cr multilayer structures were found to be coated with Ag from the bulk for growth at elevated temperatures.[24] This effect was not observed for monolayer films of Cr. Later scanning tunneling microscopy (STM) work showed evidence that at elevated growth temperatures the Cr overlayer was covered with Ag.[25,26]

X-ray diffraction is now a well-established tool for the study of surfaces and overlayer structures and has been ex-

tended to the study of epitaxial growth in real time.[27] The penetration of the x-ray beam into the film means that there is scattering from both the surface region and the bulk. The interference in the scattered waves from the surface and the bulk provides a sensitive measure of the atomic structure at the surface, in particular the relaxation of layers normal to the surface. In a study of Fe on Cu(001),[22] it has been demonstrated that the stoichiometry of the outermost layers can also be determined by this method.

We report here a study of the growth and atomic structure of Cr on Ag(001) at substrate temperatures between 100 and 470 K. The results show the change in the mode of growth and provide detailed information on the atomic structure, the ordering, and the degree of intermixing.

II. EXPERIMENT

The measurements were made on beamline 9.4 of the Synchrotron Radiation Source at Daresbury Laboratory using a five-circle surface x-ray diffractometer. X rays of wavelength 0.9 Å from the 5 T wiggler were selected by a Si(111) monochromator.[28] The scattered x-ray intensity was recorded with a cooled germanium detector mounted behind two sets of four-jaw slits to define the angular resolution. The range of accessible momentum space was increased by moving the detector out of the vertical scattering plane.[29]

The silver crystal sample, $8\times8\times3$ mm^3, was mounted in an ultrahigh-vacuum environmental chamber, coupled to the diffractometer.[30] The chamber had a large Be window and an electron analyzer for measuring the Auger electron spectroscopy (AES). The Ag crystal was cleaned in vacuum by repeated cycles of argon-ion bombardment and annealing to 600 °C until no contamination could be detected by AES. Cr was deposited from a Knudsen cell that was surrounded by a water-cooled shroud. The pressure in the chamber was 8×10^{-11} mbar, it rose to 1×10^{-10} mbar during evaporation. The growth was monitored in real time using AES and x-ray reflectivity; the coverage was subsequently confirmed using Rutherford back scattering (RBS).[31] Typical deposition rates were 20 min/ML; one monolayer (ML) is defined as the areal density of a single (001) plane of bulk Ag: 12.0×10^{14} at. cm^{-2}.

The atomic arrangement of the surface and overlayer is described by a tetragonal unit cell defined by three orthogonal base vectors that are related to the conventional cubic coordinate system of the Ag substrate by

$$\mathbf{a}_1=\frac{a_0}{2}[1\bar{1}0]_{\text{cubic}},\quad \mathbf{a}_2=\frac{a_0}{2}[110]_{\text{cubic}},\quad \mathbf{a}_3=a_0[001]_{\text{cubic}},$$

with $|\mathbf{a}_1|=|\mathbf{a}_2|=a_0/\sqrt{2}$ and $|\mathbf{a}_3|=a_0$, where a_0 is the lattice constant of Ag (4.086 Å). With this convention, the reciprocal-lattice vectors $\mathbf{b}_1$ and $\mathbf{b}_2$ are parallel to the surface and $\mathbf{b}_3$ is directed normal to the surface. The momentum transfer is given by $\mathbf{Q}=h\mathbf{b}_1+k\mathbf{b}_2+l\mathbf{b}_3$.

Specular reflectivity was measured by symmetrically increasing the incoming and outgoing angles to the surface of the crystal. Crystal truncation rods (CTR's) were measured by keeping the outgoing angle constant (1°). In this geometry the resolution of the measurement of the rod is constant. The integrated intensities were obtained by rotating the crystal about the surface normal. The structure factor amplitudes were derived by taking the square root of the integrated intensities and correcting for the variation of the footprint on the sample of the incident beam as a function of the incoming grazing angle, the polarization, and the Lorentz factor.[32] Analysis of the CTR's was achieved by using the code ROD.[33]

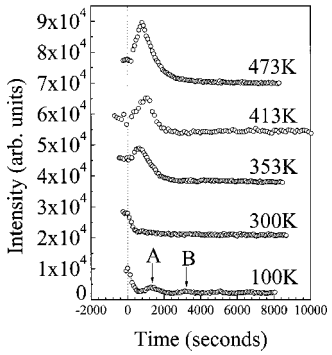

FIG. 1. The change in the intensity of the (001) position of reciprocal space with time for the deposition of Cr on Ag(001). The substrate temperature is indicated for each plot. A and B denote the first and second maxima in the low-temperature growth curve, which correspond to 2 and 5 ML, respectively.

III. RESULTS

A. Growth

Figure 1 shows the variation of the specularly reflected x-ray intensity with deposition for substrate temperatures between 100 and 470 K. The x-ray signal was recorded at a grazing angle of 6.32°, which corresponds to a scattering vector at the (001) point in the reciprocal lattice of the fcc structure of Ag. With this geometry, scattered waves from adjacent planes parallel to the surface are out of phase, thus giving the maximum sensitivity to the formation of monolayer thick islands.

The plots show a distinct change with temperature. At 100 K the intensity falls rapidly and then shows weak and rapidly decaying oscillations. Such behavior is typical of a poorly ordered layer-by-layer mode. The peaks mark the completion of different layers; the rapid decay in their height is an indication of increased roughening as a consequence of a low surface mobility. It is noted that the most obvious of the peaks, shown as A and B, occur at coverages close to 2 and 5 ML. At room temperature, the intensity again falls abruptly but, in spite of the expected increased mobility, there is no evidence of any maxima. At substrate temperatures above room temperature, the intensity shows a noticeably different variation with time. The signal initially rises to a peak and falls to a low value. RBS analysis showed that the maximum observed at 473 K corresponded to a coverage of 0.98 ± 0.05 ML.

The clear difference in the plots shown in Fig. 1 confirms that a single model cannot explain the growth process at all temperatures. The lower surface free energy of Ag compared

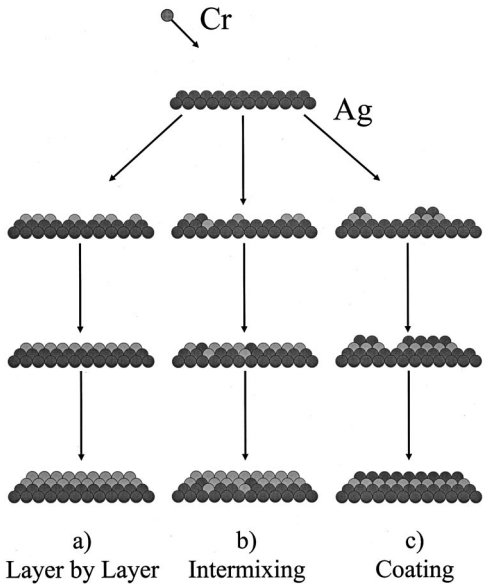

FIG. 2. Three simple models of the growth of Cr on Ag(001). (a) Layer-by-layer growth of pure Cr on Ag(001), (b) layer-by-layer growth with intermixing of the two species at the interface, and (c) overcoating of the initial Cr monolayer islands with Ag.

to that of Cr implies that simple layer-by-layer growth of Cr on the Ag substrate is unlikely and if there is enough energy to overcome the diffusion barrier, the substrate atoms will tend to replace the adsorbate atoms. Earlier results for the growth of Fe on Cu(001) (Ref. 22) showed intermixing of the atomic species, although, as in this case, the miscibility in the bulk is negligible and the crystallographic structures are well matched.

To describe the growth of Cr on Ag(001) we have considered three simple models as shown schematically in Fig. 2. They are (i) layer-by-layer growth of pure Cr on the Ag(001) substrate, (ii) layer-by-layer growth with intermixing of the two species at the interface, and (iii) overcoating of the initial Cr islands with Ag. Model (ii) is the same as that used to describe the behavior of Fe on Cu(001).[22] Model (iii) differs from the other two in that the initial growth involves the formation of a bilayer on top of the original Ag substrate. Each deposited Cr atom is immediately covered by a Ag atom that has migrated from a step or other defect on the surface. Both (ii) and (iii) lower the surface free energy.

Within the kinematical approximation, the total amplitude of the specular x-ray scattering can be expressed as a sum of contributions from individual layers,

$$F_{00l}^{\text{total}} = F_{00l}^{\text{bulk}} + \sum_n \theta_n [(1-x_n) f^{\text{Cr}} + x_n f^{\text{Ag}}] \exp(2\pi i l z_n / a_3). \tag{1}$$

Here θ_n is the fractional coverage and x_n is the fraction of Ag atoms in the nth layer; f^{Cr} and f^{Ag} are the atomic form factors of Cr and Ag. For simplicity it is assumed that the Cr and Ag atoms are at the same height z_n within a given layer. The sum is over all adsorbate and intermixed layers of the substrate. If we ignore effects due to absorption the contribution of the *undisturbed* bulk, in which layers repeat with a period $a_0/2$, is given by

$$F_{00l}^{\text{bulk}} = \frac{f^{\text{Ag}}}{1-\exp(-\pi i l)}. \tag{2}$$

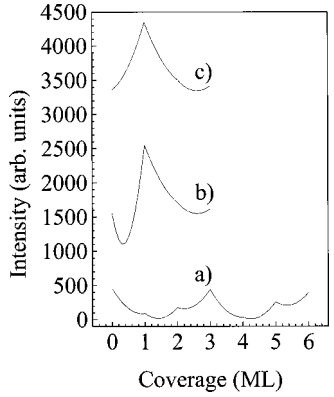

FIG. 3. The predicted variation of the reflected x-ray intensity for the three models shown in Fig. 2. The middle curve corresponds to complete exchange of the first Cr layer with the topmost Ag layer.

Figure 3(a) shows the results expected for perfect layer-by-layer growth of Cr with no intermixing. Here, $x_n = 0$ for all layers above the undisturbed Ag(001) substrate and $\theta_n = 1$ in all but the topmost Cr layer. The heights z_n were assigned by assuming that there was perfect epitaxy of a bcc Cr structure on top of the Ag(001) substrate and by using the bulk atomic diameters for Ag (2.89 Å) and Cr (2.50 Å). The vertical separation between the topmost Ag layer of the substrate and the first Cr layer is thus 1.76 Å, and the separation between Cr layers is 1.44 Å, as in the bulk. The contraction of the interlayer spacing due to perfect matching with the substrate is 0.3%, or less than 0.01 Å.

The growth curve shows a series of cusps, each corresponding to the completion of a layer. Unlike the case for perfect homoepitaxial growth for which Eq. (1) predicts a series of identical parabolas, each falling to zero at half integral coverage and reaching the same height at integral values of θ_n, the result in this case is more complex. The curve does not reach zero at each half monolayer coverage and the cusps are at different heights. In Fig. 3(a) the highest cusps occur at 3 and 6 ML coverage and the one at 4 ML is barely discernible. This is a direct result of the difference in the atomic form factor of Cr (atomic number 24) and Ag (atomic number 47), and the differences in the adsorbate and substrate layer spacings. Figure 4 shows the effect of changing the spacing between the topmost Ag layer of the substrate and the first Cr layer at the interface. The middle curve ($\delta = 0$) is the result predicted for the interface spacing of 1.76 Å; the other curves correspond to small expansions or contractions of the interface spacing. The change of phase of the overlayer wave that this movement produces alters the relative height of the peaks and the depth of the minima. In particular, when the interface spacing is increased by $\delta = 0.44$ Å, the maximum values are found to occur at 2 and 5

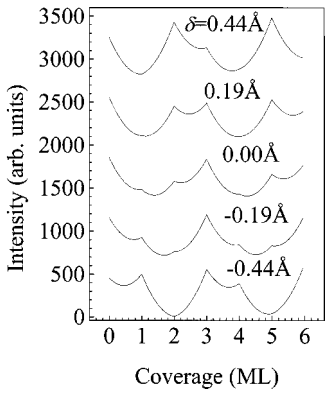

FIG. 4. The growth curves predicted for perfect epitaxial growth. The values of δ correspond to the change in interface separation relative to the hard-sphere value of 1.76 Å. The values of δ have been chosen for comparison to later fit results.

ML, as was observed in the growth curve at 100 K (Fig. 1). The cusps at 1, 3, and 4 ML are weak and would be difficult to identify in the measured plot.

Progressive roughening of the growing layer would impose a steady decay on the plots and weak features would not be discerned. This can explain the curve recorded at 300 K but cannot describe the plots recorded at higher temperatures. Contrary to the prediction of the simple model, these show an initial increase in signal.

Increasing the temperature will increase the probability of intermixing at the interface between the topmost Ag layer of the substrate ($n=0$) and the first Cr layer ($n=1$). We have calculated the effect of this by setting $1-x_0=x_1$ and keeping $x_{n>1}=0$. The degree of intermixing is determined by the value of x_1. Increasing x_1 increases the height of the first peak. The curve shown [Fig. 3(b)] corresponds to the extreme case of $x_1=1$, that is, the complete exchange of the Ag and Cr layers at the interface. It predicts the occurrence of a strong peak at 1 ML but still shows an initial fall of the intensity, contrary to the higher-temperature measurements.

The initial fall in the intensity occurs with simple layer-by-layer growth because (at the anti-Bragg position) the waves scattered from the new monolayer are out of phase with the waves scattered from the substrate. An initial increase in the signal, as seen at the higher temperatures, would occur if each monolayer island of Cr was overcoated immediately with a monolayer of Ag. The scattered waves from the heavier additional Ag layer would then be almost in phase with the scattering from the substrate, therefore increasing the total amplitude. The additional Ag atoms could diffuse from other regions of the surface. The top curve, Fig. 3(c), is the prediction of such a model. It shows the observed rise to a peak at 1 ML. The fall after the peak is due to the subsequent growth being one monolayer thick and would occur if, as shown here, the further layers were of Cr or if Ag diffused vertically to reduce the surface energy.

B. Rod scans

Measurements at one value of the momentum transfer **Q** provide only a limited picture of the structure of the films. More detail was obtained by interrupting the growth and then scanning along the $(00l)$, $(10l)$, and $(11l)$ crystal truncation rods (CTR's). Three different coverages were measured. Two were prepared with the sample held at 100 K; these films were grown to the first and second features in the growth curve corresponding to coverages of 2 and 5 ML. The third was grown with the sample at 430 K to the peak in the growth curve at 1 ML.

The measured rods were fitted using the three-dimensional form of Eq. (1) and included Debye-Waller correction factors. The Debye-Waller parameters were held at the bulk values for Cr and Ag and the substrate was assumed to be unrelaxed. Initially the Cr atoms were placed in the bcc structure with perfect in-plane registry with the substrate. That is, the interface separation was set at 1.76 Å and the separation of the Cr layers was 1.44 Å. In the fitting, the occupancy and the height of the Cr layers were allowed to relax.

To limit the number of variables in the fit, we followed the usual practice of describing a rough surface with a parametrized model for the occupancy. Such models that have been employed in earlier reports include the beta roughness model,[34] the Poisson model, the linear model, and the sinusoidal model.[35,36] They are normally used to describe clean surfaces and involve many layers. They do not, therefore, give a good representation of the low-temperature films, the growth of which is best described as a poorly defined layer-by-layer mode, that is, when the growth of one layer begins before the completion of the previous layer. In such a structure, the layers near the substrate will be complete and only the upper layers will contribute to the roughness. A better function in this case is

$$\theta_n=\left[1+\exp\left(\frac{n-N-0.5}{\alpha}\right)\right]^{-1}. \tag{3}$$

Here N is the total coverage in monolayers and α the roughness parameter. $\alpha=0$ describes a perfectly flat layer completely occupied up to the Nth layer. Increasing α will redistribute atoms to higher levels and increase the roughness; the occupancy of lower levels will remain close to unity. The constant 0.5, in the exponent, ensures that for small α the atom redistribution is confined to the outermost occupied layer and the one immediately on top of it.

C. 100 K

Figure 5 shows the measured $(00l)$, $(01l)$, and $(11l)$ rods for the 2 ML coverage. The best fits are shown by the continuous lines; the fitting parameters are listed in Table I. It was assumed that at the low temperature, intermixing would be negligible. Since the specular $(00l)$ rod is sensitive to all the atoms in the overlayer and the nonspecular $(10l)$ and $(11l)$ are sensitive only to the atoms in epitaxial positions, the nonspecular rods were fitted with the layer occupancies corrected by a factor σ.

The high level of disorder, which was evident from the growth curve shown in Fig. 1, is reflected in the relatively high occupation of the third, nominally empty, layer. It is also confirmed by the value of σ, which suggests that nearly

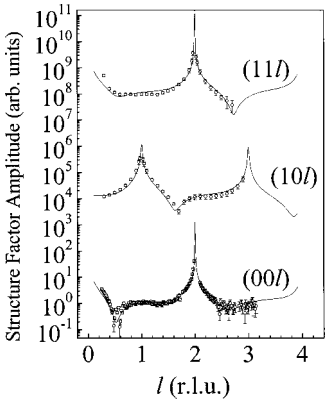

FIG. 5. Crystal truncation and specular rods measured for the 2 ML coverage grown at 100 K. The solid lines are the best fits obtained with the parameters listed in the upper part of Table I. The plots are displaced vertically for clarity.

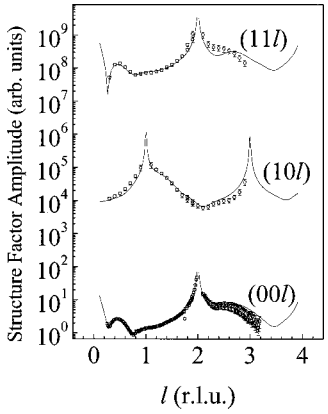

FIG. 6. Crystal truncation and specular rods measured for the 5 ML coverage grown at 100 K. The solid lines are the best fits obtained with the parameters listed in the lower part of Table I. The plots are displaced vertically for clarity.

half of the adsorbate atoms are in nonepitaxial positions. If all the atoms were in epitaxial positions, the $(00l)$ rod should have the same shape as the $(11l)$ rod on this surface. From Fig. 5 it is evident that this is not the case. The best fit with a $\chi^2=2.63$ was achieved with an interface separation expanded from the predicted value of 1.76 by 0.44 ± 0.10 Å. The fit was not improved by including the other Cr layers.

Figure 6 shows the measured rods with the best fits for the 5 ML coverage. The total number of layers used was nine. The results of the best fit are shown in Table I. The fit was improved by including an expansion of the interface spacing (0.19 ± 0.12 Å). Although the $(11l)$ and $(00l)$ rods are similar for this coverage, an occupancy factor σ of 0.8 ± 0.1 improved the fit ($\chi^2=2.09$), indicating, as in the 2 ML film, that part of the film has atoms in nonepitaxial positions.

D. 430 K

The $(00l)$ rod and the best fit for the 1 ML film grown at the higher temperature is shown in Fig. 7. Following the results obtained from the high-temperature growth curves the starting point for the fit was a monolayer of Cr atoms sandwiched between the substrate and a complete monolayer of Ag atoms. The separation of the Cr layer from each neighboring layer was therefore set initially at 1.76 Å. By allowing the heights of the two layers to vary a best fit with a $\chi^2=5.58$ was obtained. This was improved significantly by allowing atom exchange between the topmost Ag layer of the substrate and the Cr layer. The lowest $\chi^2=2.28$ was achieved with a degree of 22 ± 13 % exchange. The initial positions of the layers were set at those calculated from using the average intralayer atomic radius. The separation of the Cr layer from the substrate increased by 0.11 ± 0.12 Å and that between the Cr and the outer Ag layer by 0.31 ± 0.10 Å (see Table II).

IV. DISCUSSION

In all of the measured films the best-fit results involve expanded interlayer spacings compared to those calculated from a model involving hard-sphere radii of the two atomic species. In addition the features in the low-temperature growth curve are supported by expanded spacings at the interface. Previous work has found enhanced magnetic moments in thin Cr films. This is due to the more atomic nature of the Cr atoms favoring a more parallel configuration of the atomic spins. The interlayer spacings indicate an increase in atomic volume in the thin films, which contributes to an increase in the magnetic moments.

The results of the fits to the rods for the low-temperature films indicate disorder. It would be reasonable to assume that the epitaxy is not perfect and the Cr film relaxes to its bulk

TABLE I. Results of the best fits to the rod data for the coverages grown at liquid-nitrogen temperatures. The parameters are $\Delta z_{0,1}$, the interface spacing, σ is the crystalline fraction, and α and N the parameters for Eq. (3). Also shown are the values of the layer occupancies θn for the corresponding values of N and α. The first and second rows show the parameters for the 2 and 5 ML coverages, respectively.

2 ML	$\Delta z_{0,1}=0.44\pm0.10$, $\sigma=0.5\pm0.1$, $\alpha=0.3\pm0.1$, $N=2$								
	θ_1	θ_2	θ_3	θ_4					
	0.99	0.84	0.16	0.01					
5 ML	$\Delta z_{0,1}=0.19\pm0.12$, $\sigma=0.8\pm0.1$, $\alpha=0.7\pm0.1$, $N=5$								
	θ_1	θ_2	θ_3	θ_4	θ_5	θ_6	θ_7	θ_8	θ_9
	1.00	0.99	0.97	0.90	0.67	0.33	0.11	0.03	0.01

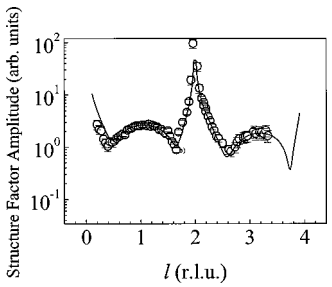

FIG. 7. The $(00l)$ rod measured for the 1 ML coverage grown at 430 K. The solid line is the best fit obtained with the parameters listed in Table II.

structure so that only a fraction of the scattering from the overlayer is coherent with that of the substrate. Since the 2 ML film has 0.5 of its atoms in epitaxial positions and the 5 ML film has 0.8, this cannot be true. It is more likely that growth commences with small islands, some of which are randomly oriented. In later stages of growth, islands that are epitaxial grow at an increased rate at the expense of the randomly orientated islands. As the islands get bigger, Cr atoms have smaller distances in which to diffuse to preferential sites.

The surface coating of the 1 ML film grown at 430 K is a consequence of the enhanced mobility of Ag atoms and their lower surface free energy compared to that of Cr. The Ag atoms involved are likely to come from steps edges on the surface. This same growth mode has been reported for Rh on Ag(001),[37] Ag on Pb(111),[38,39] Cu on Pb(111),[39] and Fe on Au(100).[40,41] In all of these cases the mechanism of the growth is thought to be driven by the difference in the surface free energies. They all result in sandwich-type structures and likewise the result of the growth in this experiment should be a Ag/Cr/Ag(001) sandwich structure. This is consistent with what we observe. Moreover, the vast improvement in the fit of the $(00l)$ rod, caused by allowing a degree of interchange between the two outer layers, cannot be ignored. This mixing occurs in spite of the immiscibility of the overlayer and substrate species. Surface alloying for this system was proposed by Ortega and Himpsel.[10] Intermixing for mutually immiscible atoms has also been found to occur for other systems including Au grown on Ni(110),[21] Fe on Cu(001),[22] and Ir on Cu(001).[23] In the first two cases, the intermixing is confined to the top layer of the substrate. These results are in contradiction to the model proposed by Krembel *et al.*[17–20,24] who found that a perfect monolayer of Cr can be formed if the Ag substrate is held at temperatures between 430 and 450 K. Our results, however, are supported by STM work where evidence was found of removal of Ag atoms from step edges to cover the Cr overlayer at elevated temperatures.[25,26]

The three-dimensional character of the growth of Cr atoms at the lower temperatures poses interesting questions about the magnetic state of the film. If initial monolayer platelets were antiferromagnetic in character, then a Cr atom sitting on top of one of these platelets would be in a frustrated spin configuration. If the Cr atom had enough energy it may diffuse to the edge of the island to avoid this energetically unfavorable situation. However, due to the higher surface free energy of Cr compared to Ag, this is also energetically unfavorable. It is suggested that it is the competition between magnetic energies and diffusion energies that give rise to the sensitivity of growth with temperature. At lower temperatures the lower mobility of adatoms means that atoms grow in a three-dimensional way, whereas at higher temperatures surface diffusion allows Cr to grow flat. In the latter case the surface free energy is lowered by high mobility Ag atoms, which migrate from defects on the substrate surface to sites on top of the monolayer platelets. Although evidence of a antiferromagnetic Cr monolayer has been found to exist on Ag(001),[17–20] a polarized neutron reflection study found evidence for ferromagnetism in a Ag/Cr/Ag(001) sandwich structure consisting of 0.33 ML of Ag.[12]

TABLE II. Results for the $(00l)$ rod for the coverage grown to the maximum in the growth curve with the sample held at 430 K. The distances shown are the departures from the calculated distances assuming hard-sphere radii.

n	θ	Δz_n	$\Delta(z_n - z_{n-1})$
1 Cr	0.78 ± 0.13	0.11 ± 0.12	0.11 ± 0.12
1 Ag	0.22 ± 0.13		
2 Cr	0.22 ± 0.13	0.42 ± 0.10	0.31 ± 0.10
2 Ag	0.78 ± 0.13		

V. CONCLUSION

The growth mode of Cr on Ag(001) has been measured by surface x-ray diffraction at several different substrate temperatures. This experiment has shown the sensitivity of the growth with the temperature of the substrate. With the sample at room temperature a disordered growth mode is found while at low temperatures a poorly defined layer-by-layer growth is favored. This contrasts with growth at a higher substrate temperature where a model involving coating of platelets of Cr with Ag atoms adequately describes the variation in the (001) intensity. Some intermixing between the Cr overlayer and the Ag atoms covering the overlayer also contributes to the growth process.

Three different coverages were measured. Two were grown with the temperature of the substrate held at 100 and one at 430 K. Expanded interlayer spacings, compared to values calculated assuming a hard-sphere radius, were found in all of the films. This result is also supported by the analysis of the growth curves. The 1 ML coverage grown at 430 K was described by allowing a Ag layer to cover the Cr overlayer with an atomic interchange of $22 \pm 13\%$ between them.

ACKNOWLEDGMENT

The authors greatly appreciate the technical assistance of Stuart Thornton.

*Present address: Department of Physics and Astronomy, University of Leeds, Leeds, LS2 9IT, UK.
†Present address: ASM Europe BV, Rembrandtlaan 9, 3723 BG Biltoven, The Netherlands.

[1] U. Gradmann, J. Magn. Magn. Mater. **100**, 481 (1991).
[2] M. Wuttig, B. Feldmann, and T. Flores, Surf. Sci. **333**, 659 (1995).
[3] J. Noffke and L. Fritsche, J. Phys. C **14**, 89 (1981).
[4] G. E. Bacon, Acta Crystallogr. **14**, 823 (1961).
[5] C. L. Fu and A. J. Freeman, Phys. Rev. B **33**, 1755 (1986).
[6] R. H. Victoria and L. M. Falicov, Phys. Rev. B **31**, 7335 (1985).
[7] L. E. Klebanoff, S. W. Robey, G. Liu, and D. A. Shirley, Phys. Rev. B **30**, 1048 (1984).
[8] J. Schafer, Eli Rotenberg, G. Meigs, S. D. Kevan, P. Blaha, and S. Hufner, Phys. Rev. Lett. **83**, 2069 (1999).
[9] G. Allan, Phys. Rev. B **44**, 13 641 (1991).
[10] J. E. Ortega and F. J. Himpsel, Phys. Rev. B **47**, 16 441 (1993).
[11] D. A. Newstead, C. Norris, C. Binns, and P. C. Stephenson, J. Phys. C **20**, 6245 (1987).
[12] A. D. Johnson, J. A. C. Bland, C. Norris, and H. Lauters, J. Phys. C **21**, L899–L904 (1988).
[13] M. E. Haughan, Qibiao Chen, M. Onelion, and F. J. Himpsel, Phys. Rev. B **49**, 14 028 (1994).
[14] Jian-Tao Wang, Zhi-Qiang Li, Lei Zhou, Yoshiyuki Kawazoe, and Ding-Sheng Wang, Phys. Rev. B **59**, 6974 (1999).
[15] Jian-Tao Wang, Zhi-Qiang Li, and Yoshiyuki Kawazoe, J. Phys.: Condens. Matter **10**, 9655 (1998).
[16] M. Venkatraman and J. P. Neumann, Bull. Alloy Phase Diagrams **11**, 263 (1990).
[17] C. Krembel, M. C. Hanf, J. C. Peruchetti, D. Bolmont, and G. Gewinner, Solid State Commun. **81**, 219 (1992).
[18] C. Krembel, M. C. Hanf, J. C. Peruchetti, D. Bolmont, and G. Gewinner, Phys. Rev. B **44**, 8407 (1991).
[19] C. Krembel, M. C. Hanf, J. C. Peruchetti, D. Bolmont, and G. Gewinner, J. Magn. Magn. Mater. **93**, 529 (1991).
[20] C. Krembel, M. C. Hanf, J. C. Peruchetti, D. Bolmont, and G. Gewinner, Phys. Rev. B **44**, 11 472 (1991).
[21] L. Pleth Nielson, F. Besenbacher, I. Stensgaard, E. Laegsgaard, C. Engdahl, P. Stoltze, K. W. Jacobsen, and J. K. Nørskov, Phys. Rev. Lett. **71**, 754 (1993).
[22] M. A. James, Ph.D. thesis, University of Leicester, 1995.
[23] G. Gilarowski and H. Niehus, Surf. Sci. **436**, 107 (1999).
[24] C. Krembel, M. C. Hanf, J. C. Peruchetti, D. Bolmont, and G. Gewinner, J. Vac. Sci. Technol. A **10**, 3325 (1992).
[25] A. J. Quinn, J. F. Lawler, R. Schad, and H. van Kempen, Surf. Sci. **385**, 395 (1997).
[26] J. F. Lawler, R. G. P. van der Kraan, H. van Kempen, and A. J. Quinn, J. Magn. Magn. Mater. **165**, 195 (1997).
[27] C. Norris, Philos. Trans. R. Soc. London, Ser. A **344**, 557 (1993).
[28] C. Norris, M. S. Finney, G. F. Clark, G. Baker, P. R. Moore, and R. G. van Silfhout, Rev. Sci. Instrum. **63**, 1083 (1992).
[29] J. S. G. Taylor, C. Norris, E. Vlieg, M. Lohmeier, and T. S. Turner, Rev. Sci. Instrum. **67**, 2658 (1996).
[30] C. L. Nicklin, J. S. G. Taylor, N. Jones, P. Steadman, and C. Norris, J. Synchrotron Radiat. **5**, 890 (1998).
[31] RBS analysis was carried out by C. Jeynes and N. Barradas at the University of Surrey, England.
[32] E. Vlieg, J. Appl. Crystallogr. **30**, 532 (1997).
[33] E. Vlieg, J. Appl. Crystallogr. **33**, 401 (2000).
[34] I. K. Robinson, Phys. Rev. B **33**, 3830 (1986).
[35] M. Lohmeier, S. de Vries, J. S. Custer, E. Vlieg, M. S. Finney, F. Priolo, and A. Battaglia, Appl. Phys. Lett. **64**, 1803 (1994).
[36] D. Stearns, J. Appl. Phys. **65**, 491 (1989).
[37] P. J. Schmitz, W. Y. Leung, G. W. Graham, and P. A. Thiel, Phys. Rev. B **40**, 11 477 (1989).
[38] C. H. Chen and F. J. Sansalone, Surf. Sci. **164**, L688 (1985).
[39] K. J. Rawlings and P. J. Dobson, Thin Solid Films **67**, 171 (1980).
[40] S. D. Bader and E. R. Moog, J. Appl. Phys. **61**, 3729 (1987).
[41] V. Blum, Ch. Rath, S. Muller, L. Hammer, K. Heinz, J. M. Garcia, J. E. Ortega, J. E. Prieto, O. S. Hernan, J. M. Gallego, A. L. Vázquez de Parga, and R. Miranda, Phys. Rev. B **59**, 15 966 (1999).